HHS Public Access

Author manuscript

Gastroenterology. Author manuscript; available in PMC 2017 June 01.

Published in final edited form as:

Gastroenterology. 2016 June ; 150(7): 1659–1672.e5. doi:10.1053/j.gastro.2016.02.070.

Radiation Therapy Induces Macrophages to Suppress Immune Responses Against Pancreatic Tumors in Mice

Lena Seifert[1], **Gregor Werba**[1], **Shaun Tiwari**[1], **Nancy Ngoc Giao Ly**[1], **Susanna Nguy**[2], **Sara Alothman**[1], **Dalia Alqunaibit**[1], **Antonina Avanzi**[1], **Donnele Daley**[1], **Rocky Barilla**[1], **Daniel Tippens**[1], **Alejandro Torres-Hernandez**[1], **Mautin Hundeyin**[1], **Vishnu R. Mani**[1], **Cristina Hajdu**[3], **Ilenia Pellicciotta**[3], **Philmo Oh**[2], **Kevin Du**[2], and **George Miller**[1,4]

[1]S. Arthur Localio Laboratory, Dept. of Surgery, New York University School of Medicine, 550 First Avenue, New York, NY 10016

[2]S. Arthur Localio Laboratory, Dept. of Radiation Oncology, New York University School of Medicine, 550 First Avenue, New York, NY 10016

[3]S. Arthur Localio Laboratory, Dept. of Pathology, New York University School of Medicine, 550 First Avenue, New York, NY 10016

[4]S. Arthur Localio Laboratory, Dept. of Cell Biology, New York University School of Medicine, 550 First Avenue, New York, NY 10016

Abstract

Background & Aims—The role of radiation therapy in the treatment of patients with pancreatic ductal adenocarcinoma (PDA) is controversial. Randomized controlled trials investigating the efficacy of radiation therapy in patients with locally advanced unresectable PDA have reported mixed results, with effects ranging from modest benefit to worse outcome, compared with control therapies. We investigated whether radiation causes inflammatory cells to acquire an immune-suppressive phenotype that limits the therapeutic effects of radiation on invasive PDAs and accelerates progression of pre-invasive foci.

Methods—We investigated the effects of radiation in $p48^{Cre}$;LSL-$Kras^{G12D}$ (KC) and $p48^{Cre}$;LSLKras^{G12D};LSL-$Trp53^{R172H}$ (KPC) mice, as well as in C57BL/6 mice with orthotopic tumors grown from FC1242 cells derived from KPC mice. Some mice were given neutralizing

Address correspondence to: George Miller, MD, Departments of Surgery and Cell Biology, New York University School of Medicine, 430 East 29th Street, East River Science Park, Room 660, New York, NY 10016, Tel: (646) 501-2208, Fax: (212)-263-6840, george.miller@nyumc.org.

Author Contributions: LS (acquisition of data; analysis and interpretation), GW (acquisition of data; analysis and interpretation; manuscript preparation; statistical analysis), ST (acquisition of data), NL (acquisition of data), SN (acquisition of data; analysis and interpretation), SA (acquisition of data), DA (acquisition of data), AA (technical assistance), DD (data analysis, critical review), RB (acquisition of data; manuscript preparation), DT (technical assistance), ATH (data analysis, critical review), MH (data analysis, critical review), VM (data analysis, critical review), CH (data analysis), IP (study concept and design), PO (experimental design, technical assistance), KD (study concept and design; study supervision; critical revision), GM (study concept and design; study supervision; critical revision).

Disclosure: None of the authors has any potential conflict of interest related to this manuscript.

antibodies against macrophage colony stimulating factor 1 (CSF1 or MCSF) or F4/80. Pancreata were exposed to doses of radiation ranging from 2–12 Gy and analyzed by flow cytometry.

Results—Pancreata of KC mice exposed to radiation had a higher frequency of advanced pancreatic intraepithelial lesions and more foci of invasive cancer than pancreata of unexposed mice (controls); radiation reduced survival time by more than 6 months. A greater proportion of macrophages from invasive and pre-invasive pancreatic tumors had an immune-suppressive, M2-like phenotype, compared with control mice. Pancreata from mice exposed to radiation had fewer $CD8^+$ T cells than controls and greater numbers of $CD4^+$ T cells of T-helper 2 and T-regulatory cell phenotypes. Adoptive transfer of T cells from irradiated PDA to tumors of control mice accelerated tumor growth. Radiation induced production of MCSF by PDA cells. An antibody against MCSF prevented radiation from altering the phenotype of macrophages in tumors, increasing the anti-tumor T-cell response and slowing tumor growth.

Conclusions—Radiation exposure causes macrophages in PDAs of mice to acquire an immune-suppressive phenotype and reduce T-cell mediated anti-tumor responses. Agents that block MCSF prevent this effect, allowing radiation to have increased efficacy in slowing tumor growth.

Keywords

Th2; immune regulation; pancreas; pancreatic cancer

Introduction

Pancreatic ductal adenocarcinoma (PDA) is the 4th leading cause of cancer-related death in the US with cure rates of only 1–2%[1]. Complete resection remains the only potentially curative option for PDA, but only ~15% of patients present with resectable disease. Further surgery ultimately only cures ~10% of resected patients[2]. Most patients with PDA present with locally advanced disease which is deemed unresectable on account of tumor encroachment on the portal vein or mesenteric vessels[3]. These patients are typically treated with either chemotherapy alone or chemotherapy combined with radiation therapy (RT)[4].

RT induces cancer cell death by either directly causing DNA damage or creating free radicals within tumor cells which can in turn damage the host DNA. However, the survival benefit gained from adding RT in patients with locally advanced PDA remains controversial despite five randomized clinical trials published to date[5–9]. An early Phase III study showed no benefit to adding RT to 5-FU-based chemotherapy alone, although this study has been criticized due to the use of outdated RT planning methods and a small sample size[9–11]. The first Gastrointestinal Tract Cancer Group (GITSG) trial showed a small benefit to chemotherapy + RT compared with RT alone, but this study lacked a chemotherapy only arm[5]. The second GITSG study demonstrated a significantly increased median survival of 10 months (1-year survival 41%) in the chemotherapy + RT group compared to 8 months (1-year survival 19%) in the chemotherapy only group[7]. The ECOG 4201 study similarly reported a median survival of 11.0 months for patients receiving RT + concurrent gemcitabine versus 9.2 months for the gemcitabine only group[9]. However, the FFCD/SFRO study actually demonstrated a significantly decreased median survival of 8.6 months (2-year survival 32%) in the chemotherapy + RT group compared to 13 months (2-year survival

53%) in the chemotherapy only group[8]. Collectively, these data suggest that whereas there may be clinical efficacy to RT at selected doses, fractionations, or chemotherapy combinations, the benefits are modest and select regimens may even have the potential to induce worse outcomes in locally advanced PDA patients. Moreover, the optimal treatment paradigm has yet to be defined.

Histologic analyses of both human and mouse models of PDA reveal that foci of invasive tumor are almost invariably surrounded by dysplastic PanIN lesions. Notably, PanIN lesions are ubiquitous in most persons over aged 50, even in the absence of invasive PDA[12]. Further, unlike most adenocarcinomas whose volume is comprised primarily of transformed epithelial cells, PDA is composed largely of fibro-inflammatory elements interspersed with islands of neoplastic epithelium[13, 14]. Specific peri-pancreatic leukocytic subsets, depending on their terminal differentiation phenotype, can have divergent effects on oncogenesis by either combating cancer growth via antigen-restricted tumoricidal immune responses, or by promoting tumor progression via induction of immune suppression. For example, cytotoxic $CD8^+$ T cells and Th1-polarized $CD4^+$ T cells mediate tumor protection in murine models of PDA and are associated with prolonged survival in human disease[15–17]. Accordingly, PDA-infiltrating T cells have specificity for tumor antigen[18]. However, negating cytotoxic $CD8^+$ anti-tumor responses by tumor-infiltrating myeloid-derived suppressor cells accelerates PDA development and promotes liver metastases in advanced disease[19, 20]. Similarly, $CD204^+MHCII^{low}$ M2-polarized macrophages have tumor-promoting effects in PDA by releasing immune-suppressive cytokines and inducing Th2 and Treg differentiation of $CD4^+$ T cells[21]. Consistent with these reports, we found that antigen-restricted Th2-polarized $CD4^+$ T cells promote malignant progression in mice with pre-invasive PDA[18]. Intra-tumoral $CD4^+$ Th2 cell infiltrates and $FoxP3^+$ Tregs are also associated with reduced survival in human PDA[15–17]. Collectively, these data suggest that manipulating the cellular differentiation of macrophages or $CD4^+$ T cells can affect the rate of PDA growth.

Current clinical trials studying RT in PDA are investigating the effects of intensifying radiation regimens, optimizing combinations with systemic agents, and improving patient selection. However, an opportunity exists in murine modeling to investigate mechanisms of treatment resistance to enhance therapeutic efficacy of RT. We postulated that despite the direct tumoricidal effects of RT on malignant epithelial cells, its clinical efficacy in PDA is limited by promotion of innate and adaptive immune suppression which can have the dual effects of (i) accelerating progression of invasive carcinoma and (ii) promoting oncogenic transformation in pre-invasive foci of disease. Consequently, we predicted that limiting these collateral inflammation-based pro-tumorigenic effects would enhance the efficacy of RT in pre-clinical models and human disease.

Materials and Methods

Animals and Tumor Models

C57BL/6 (H-2Kb) mice were purchased from Jackson (Bar Harbor, ME). $p48^{Cre}$;LSL-$Kras^{G12D}$ (KC; gift of Dafna Bar-Sagi, NYU) mice, which develop pancreatic neoplasia endogenously by expressing one mutant *Kras* allele in the pancreas were generated by crossing LSL-$Kras^{G12D}$ mice with $p48^{Cre}$ mice, which express Cre recombinase from a

pancreatic progenitor-specific promoter[22]. p48^{Cre};LSL-Kras^{G12D};LSL-Trp53^{R172H} (KPC; gift of Mark Philips, NYU) mice additionally express mutant *p53*[23]. For orthotopic tumor challenge, mice were administered FC1242 cells derived from pancreata of KPC mice (gift of David Tuveson, Cold Spring Harbor Laboratory). Cells were suspended in PBS with Matrigel (BD Biosciences) at 10^6 cells/mL and 5×10^4 cells were administered into the body of the pancreas via laparotomy. In selected experiments, a neutralizing mAb targeting M-CSF (5A1, 8mg/kg) or a neutralizing mAb targeting macrophages (F4/80, 6mg/kg; both Bio X Cell) were administered daily beginning one day prior to RT and continuing until two days post-radiation. Chronic pancreatitis was induced using a regimen of seven hourly i.p. injections of caerulein (50μg/kg; Sigma-Aldrich) thrice weekly for four weeks as described[24]. Serum Amylase and Lipase levels were determined using kits (Sigma-Aldrich). For serum cytokine analysis, a cytometric bead array was used according to the manufacturer's protocol (BD Biosciences). All procedures were approved by the NYU School of Medicine IACUC.

RT of murine PDA

In our orthotopic PDA model, one day prior to RT (day 18) animals underwent a mini-laparotomy with fiducial placement surrounding the tumor to mark the target area for RT (Premium Surgiclip, Covidien). For RT planning, a cone beam CT scan using the Small Animal Radiation Research Platform (SARRP, Xstrahl) was employed. Images were transferred into Slicer V3 software. Tumor-directed RT was performed using a 10x10mm collimator. In our endogenous tumor models, fiducials were placed in the peri-pancreatic adipose tissue in 6 week-old KC mice or 1 month-old KPC mice. RT was targeted in a similar manner. Pancreata were radiated at doses ranging from 2–12 Gy. In our fractioned RT experiments, mice were treated with 3 doses of 6 Gy at 48 hour intervals. In our Chemo-RT experiments, orthotopic tumor-bearing mice were treated with a signle dose of Gemcitabine (100 mg/kg, i.p.) one day prior to hypofractionated RT (12 Gy).

Cellular isolation & flow cytometry

Pancreata were harvested immediately after mouse sacrifice and placed in RPMI1640 with 1 mg/mL Collagenase IV (Worthington Biochemical) and 1 U/mL DNAse I (Promega). After mincing with scissors, tissues were incubated at 37°C for 30 minutes with gentle shaking. Specimens were filtered and then centrifuged at 350g for 5 minutes. Cell pellets were resuspended in PBS with 1% FBS. After blocking FcγRIII/II (αCD16/CD32, eBioscience), cell labeling was performed by incubating 10^6 cells with 1 μg of fluorescently conjugated antibodies directed against CD45 (30-F11), MHC II (M5/114.15.2), CD11b (M1/70), F4/80 (BM8), Gr1 (RB6-8C5), CD204 (2F8), CD206 (C068C2), PD-L1 (10F.9G2), CSFR1 (AFS98), CD40 (3/23), CD3 (17A2), CD4 (RM4-5), CD8 (53-6.7), FoxP3 (150D), CD25 (PC61), CD44 (IM7), IL-10 (JES5-16E3), and TNF-α (MP6-XT22; all Biolegend). Intracellular cytokine staining was performed using the BD FixPerm Kit (BD Biosciences). Flow cytometry was performed on the LSR-II (BD Biosciences). Data were analyzed using FlowJo software.

Western blotting

For protein extraction, 15–30 mg of tissue were homogenized in 150–300μL tissue lysis buffer, incubated for 30 minutes on ice, centrifuged at 14,000g for 15 minutes, followed by supernatant collection. Total protein was quantified using the BioRad DC Protein Assay (BioRad). Western blotting was performed as per our previously described protocols with minor modifications[25]. Briefly, 10 % Bis-Tris polyacrylamide gels (NuPage, Invitrogen) were equiloaded with 10–30μg of protein, electrophoresed at 200 V, and electrotransferred to PVDF membranes. After blocking with 5% BSA, membranes were probed with primary antibodies to β-actin (Abcam), NF-κB/p65, p-NF-κB/p65, Erk1/2, p-Erk1/2, STAT3, and p-STAT3 (all Cell Signaling). Blots were developed by ECL (Thermo Scientific).

Histology & Immunohistochemistry (IHC)

For histological analysis, pancreatic specimens were fixed and embedded with paraffin, and stained with Trichrome or H&E. The fraction of fibrotic area was calculated based on Trichrome staining using a computerized grid as previously described[25]. The fraction and number of ducts containing ADMs, all grades of PanIN lesions or invasive carcinoma was morphologically determined by examining a minimum of 10 HPFs/slide by a blinded pathologist. ADMs were defined morphologically as acinar complexes having a circular morphology with a central lumen but lacking columnar architecture. PanINs were graded according to established criteria[26]. Briefly, In PanIN I ducts, the normal cuboidal pancreatic epithelial cells transition to columnar architecture (PanIN Ia) and gain polyploid morphology (PanIN Ib). PanIN II lesions are associated with additional nuclear abnormalities such as loss of polarity. PanIN III lesions, or in-situ carcinoma, show cribriforming, budding off of cells, and luminal necrosis with marked cytological abnormalities, without invasion beyond the basement membrane. Loci of frank carcinoma were identified by invasion beyond the basement membrane. The percentage of ducts in pancreata of KC mice containing normal morphology, ADM, graded PanIN lesions was determined as a fraction of all ducts on a given slide. In select experiments the total number of invasive foci per longitudinal section of paraffin-embedded pancreas was recorded. Each pancreas was examined a 2 levels of depth by H&E. IHC was performed using antibodies directed against Amylase, α-SMA, CD45 (all polyclonal), F480 (CI:A3-1), CD68 (KP1) and Arg1 (EPR6671(B); all Abcam), CK19 (TROMA-III; DSHB, University of Iowa), CD4 (RM4-5; BD Bioscience), and M-CSF (polyclonal; Novus).

mRNA Analysis

Total RNA was extracted using the RNEasy Mini Kit (Qiagen) and converted to cDNA using the RT^2 First Strand Kit (Qiagen). qPCR was performed using the RT^2 SYBR Green qPCR mastermix (Qiagen) on the MX3005P (Stratagene). For Csf1 analysis, pre-designed primers were purchased from Qiagen. Expression levels were normalized to β-actin. For Nanostring assays, the Mouse Immunology panel was employed and data analyzed using the nCounter System (Nanostring).

T cell adoptive transfer experiments and PDA-macrophage co-culture assays

For T cell adoptive transfer experiments, $CD3^+$ T cells from RT (12 Gy) or sham-treated orthotopic tumors were FACS-sorted (SY3200, Sony) and co-injected subcutaneously into mice in a 1:10 ratio with KPC-derived tumor cells (1×10^6) or Pan02 cells (5×10^6; gift of Daniel Meruelo, NYU). For PDA-macrophage co-culture assays, KPC-derived tumor cells (5×10^4) were irradiated at 12 Gy. One hour later, FACS-sorted macrophages were added to the cancer cells (2:1 ratio). After 48 hours, macrophages were harvested and analyzed by flow cytometry.

In vitro T cell activation assays

For T cell activation assays, mouse $CD3^+$ T cells (5×10^4) were plated in 96 well plates coated with anti-CD3 (145-2C11, 10μg/ml) and anti-CD28 (37.51; 10μg/ml, both Biolegend) either alone or with macrophages (5:1 ratio) harvested from RT- or sham-treated orthotopic tumors. After 72 hours, T cells were harvested and analyzed for expression of TNF-α by flow cytometry.

Statistical Analysis

Data is presented as mean +/− standard error. Survival was measured according to the Kaplan-Meier method. Statistical significance was determined by the Student's *t* test and the log-rank test using GraphPad Prism. P-values <0.05 were considered significant.

Results

Hypofractionated RT accelerates the progression of pancreatic dysplasia to invasive carcinoma

To test the effects of RT on modulating tumorigenesis, 6 week old KC mice which exhibit scattered early PanIN lesion (Figure S1a) were administered pancreas-directed RT (12Gy) and analyzed for tumor progression 8 weeks later. Pancreata of RT-treated mice displayed accelerated tumorigenesis as evidenced by a higher frequency of advanced PanIN lesions as well as numerous foci of invasive cancer (Figure 1a). RT-treated pancreata also exhibited a concomitant dense fibro-inflammatory desmoplasia with higher staining for Collagen (Figure 1b) and α-SMA (Figure 1c), indicative of stellate cell activation. Further, RT-treated mice demonstrated a ~8 month reduction in median survival (Figure 1d). Dose response experiments revealed that 2Gy had a negligible effect on tumor progression whereas doses of 6Gy or higher were progressively oncogenic (Figure S1b, c). RT did not induce higher NF-κB or MAP kinase signaling in PDA (Figure 1e). Consistent with the lack of induction of pro-inflammatory signaling, RT did not influence disease phenotype in WT pancreata in the setting of caerulein-induced chronic pancreatitis nor did it alter pancreatic architecture in WT mice after PBS administration (Figure S2).

RT induces an immune-suppressive macrophage phenotype

We hypothesized that RT accelerates oncogenic changes in pre-invasive pancreata by inducing tumor-promoting inflammation. However, consistent with the absence of higher inflammatory signaling in RT-treated KC mice, we found that the immune infiltrate in

control and RT-treated KC animals was similar at 8 weeks post-treatment (Figure S3). Therefore, we postulated that critical changes were occurring in the pre-malignant pancreas in the early aftermath of RT. Consistent with this hypothesis, the number of intra-pancreatic $CD45^+$ pan-leukocytes increased markedly by 3 days after RT (Figure 2a). Similarly, RT was associated with increased early infiltration of $F4/80^+$ tumor-associated macrophages (TAMs) and $Arg1^+$ leukocytes (Figure 2a). To assess the phenotype of TAMs in RT-treated pancreata, we performed mRNA analysis. RT induced a reduction in *iNos*, *Irf5*, and *H2eb1* expression but upregulation in *Arg1*, consistent with M2-like macrophage differentiation (Figure 2b). Further, RT increased STAT3 phosphorylation (Figure 2c), diminished MHCII expression in TAMs (Figure 2d), and increased TAM expression of CD206, PD-L1, and CSFR1, but modestly diminished CD40 expression (Figure 2e). Collectively, these data suggest that RT reprograms PDA-infiltrating TAMs toward an M2-like phenotype. However, in departure from the classical M2 description, TNF-α was sharply upregulated in TAMs after RT (Figure 2f).

RT treatment of invasive PDA increases infiltration of M2-polarized TAMs

To determine whether RT similarly induces M2 reprogramming of macrophage populations in invasive PDA, we performed RT on mice bearing KPC-derived orthotopic pancreatic tumors before assessing TAM phenotype on day 3. Unlike pre-invasive lesions, RT predictably but modestly reduced the growth rate and induced tumor necrosis in invasive PDA (Figure 3a). However, similar to pre-invasive PDA, tumor infiltration by TAMs was substantially increased after RT treatment (Figure 3b). Further, TAMs exhibited similar M2 reprogramming as evidenced by reduced MHC II expression but higher CD204 and CD206 expression (Figure 3b). $Arg1^+$ cell infiltration was also increased after RT (Figure 3c). Administration of fractionated RT or Gemcitabine-based Chemo-RT similarly induced M2 reprogramming of TAMs (Figure S4a, b). To investigate whether RT induction of a M2-polarized TAM phenotype in PDA is affected by the extent of transformation, we treated KPC mice with RT and directly compared MHC II expression in TAMs between invasive and pre-invasive regions of pancreata. We found that whereas MHCII expression was diminished in PDA-infiltrating TAMs in all locations, it was reduced to a significantly greater extent in pre-invasive areas (Figure 3d).

We postulated that irradiated PDA cells secrete factors which promote the distinct M2-like differentiation of macrophages seen in our tumor models. To test this, we co-cultured naïve splenic macrophages *in vitro* with irradiated or sham-treated KPC-derived tumor cells. Irradiated tumor cells induced an increased $MHCII^{low}CD204^{high}TNF\text{-}\alpha^+$ macrophage phenotype suggesting that irradiated PDA cells can directly promote the distinct TAM phenotype associated with RT therapy in PDA (Figure 3e, f).

RT-induced M-CSF expression from tumor cells drives TAM infiltration and M2-deviation

Since M-CSF can expand macrophage populations and drive M2 differentiation[27], we postulated that RT upregulates M-CSF expression in PDA cells. We found a ~5-fold increase in M-CSF expression in PDA after RT treatment by PCR in KPC orthotopic tumors (Figure 4a). Immunohistochemical analysis confirmed elevated M-CSF expression in transformed pancreatic ductal cells on day 3 after RT in KC pancreata (Figure 4b). M-CSF was not

residually elevated at 8 weeks after treatment (not shown). Moreover, M-CSF blockade reduced TAM infiltration in RT-treated PDA and reversed their M2 reprogramming (Figure 4c). We predicted that M-CSF blockade would enhance the anti-tumor efficacy of RT in PDA. To test this, cohorts of mice bearing orthotopic KPC-derived tumor were treated with a neutralizing α-M-CSF mAb or isotype control coincident with RT administration. Again, RT alone had only modest effects on slowing tumor growth. Similarly, α-M-CSF administration alone was ineffectual. However, RT + α-M-CSF treatment offered marked tumor protection (Figure 4d). Similarly, macrophage neutralization coincident with RT using an α-F4/80 mAb also significantly enhanced the radiation effect (Figure 4e). To determine whether M-CSF blockade could mitigate the RT-induced accelerated oncogenesis in pre-invasive foci of PDA, we administered α-M-CSF treatment for 3 days surrounding RT treatment of 6 week-old KC mice and scarified animals 2 months later. Consistent with the beneficial effects of concomitant α-M-CSF therapy in RT treatment of invasive PDA, M-CSF inhibition mitigated RT-induced disease progression in pre-invasive carcinoma (Figure S5).

T cells from irradiated PDA promote tumor growth

Since M2-polarized macrophages can induce T cell anergy, we postulated that the mechanism for the accelerated tumorigenesis in RT-treated KC pancreata was related to ineffectual adaptive immunity. We interrogated T cell phenotype in pancreata of KC mice 3 days after RT- or sham-treatment. The fraction of $CD3^+$ T cells within the TME was significantly decreased in RT-treated pancreata (Figure 5a). Moreover, the CD4:CD8 ratio and the total number of $CD4^+$ T cells increased with RT (Figure 5a, b). $CD4^+$ T cells have recently been reported to promote pancreatic tumorigenesis and we, and others, specifically implicated Th2 cells and Tregs[15, 17, 18]. We found that the immune-suppressive Th2 cytokine IL-10 was upregulated in pancreas-infiltrating $CD4^+$ T cells after RT (Figure 5c). Treatment with fractionated doses of RT also resulted in increased $CD4^+$ T cell expression of IL-10 (not shown). Further, whereas $CD4^+CD25^+FoxP3^+$ Tregs were rare in control KC pancreata, RT recruited a higher fraction of Tregs (Figure 5d) with increased IL-10 expression (Figure 5e). Additionally, examination of the tumor-infiltrating $CD8^+$ T cell fraction revealed significantly less activated cytotoxic T cells in the RT-treated cohort (Figure 5f). Collectively, these data suggest that RT results in immune suppressive T cell reprogramming in pre-invasive PDA. To directly test whether RT-entrained TAMs in PDA delimit T cell activation, we co-cultured αCD3/αCD28-stimulated splenic T cells with TAMs harvested from sham- or RT-treated PDA. Consistent with our *in vivo* data, RT-entrained macrophages diminished T cell expression of TNF-α. Moreover, the inhibitory effects were reversed by *in vivo* M-CSF blockade in the RT-treated group (Figure S6).

To investigate whether adaptive immune suppression was also associated with irradiation of invasive PDA, we again performed RT in orthotopic KPC-derived tumors and assayed T cell phenotype 3 days later. In parallel with the findings in our pre-invasive model, RT reduced the fraction of tumor-infiltrating $CD3^+$ T cells, increased the CD4:CD8 ratio, and recruited a substantially increased fraction of Tregs (Figure 6a). To determine whether the immune suppressive T cell phenotype was contingent on the M2-polarized macrophage population induced by RT, we again inhibited macrophage recruitment and M2-polarization using α-M-CSF. Concurrent blockade of M-CSF with RT reversed the diminished intra-pancreatic pan-

T cell infiltration and upregulation of Tregs associated with RT administration (Figure 6b, c).

To determine whether the T cell phenotype resulting from RT of PDA tumors is sufficient to promote oncogenic progression *in vivo*, we performed T cell adoptive transfer coincident with tumor implantation. WT mice were administered Pan02 tumor cells alone, Pan02 cells + T cells harvested from sham-treated KPC-derived tumors, or Pan02 cells + T cells harvested from RT-treated KPC-derived tumors. Remarkably, T cells derived from irradiated PDA accelerated tumor growth implying that tumor-infiltrating T cells in RT-treated PDA promote pancreatic tumor growth (Figure 6d). Similar tumor-promoting effects were observed when transferring T cells harvested from RT-treated orthotopic KPC tumors to other orthotopically implanted KPC tumor (Figure 6e). However, concurrent αM-CSF treatment of donor mice at the time of RT reversed the tumor-promoting effects of RT-entrained PDA-infiltrating T cells. α-M-CSF therapy alone did not enhance the tumor-protective properties T cells in absence of RT (Figure 6e). These data confirm that PDA-infiltrating T cells induced by RT-reprogramed macrophages promote oncogenic progression. Moreover, therapeutic inhibition of macrophage reprogramming has the potential to prevent the generation of tumor-promoting T cell populations and increase the therapeutic efficacy of RT in PDA.

Discussion

The effects of radiotherapy on the immunology of PDA have not been intensively studied. However, work in other cancers has suggested that radiation should be considered an immune adjuvant as evidenced by RT-induced enhancement of both innate and adaptive immunity. For example, the immunogenicity of dendritic cells (DC) is reportedly improved by radiation-induced necrotic tumor cell release of HMGB1 which ligates TLR4 and TLR9 on DC thereby promoting their cellular maturation and enhancing their antigen processing capabilities[28]. Another consequence of radiation-induced necrotic cell death is the translocation of calreticulin (CRT) from the endoplasmic reticulum to the plasma membrane which facilitates assembly of MHC I-peptide complexes[29]. CRT also enhances DC cross presentation of antigens to cytotoxic T lymphocytes[30]. In addition to upregulating the antigen-presentation machinery in DC, radiation can reportedly enhance immunogenicity by inducing the release of tumor antigens, upregulating the expression of T-cell co-activating ligands, and sensitizing tumor cells to antigen-independent cell death via the Fas receptor[31]. Radiation is further thought to augment diverse aspects of T cell immunity via adenosine triphosphate release from apoptotic cells which induces secretion of IL-1β[32]. A consequence of this cascade is Th1 polarization of antigen-restricted $CD4^+$ T cell responses and activation of γδ T cells[33]. Additionally, tumoricidal γδ T cells can be further activated by irradiation via NKG2D receptor recognition of stress-ligand expressing cancer cells[34].

Despite sufficient evidence for immunogenic influences of radiation in extra-pancreatic malignancies, our data suggests that RT in PDA leads to pronounced immune-suppression within the TME via expansion of immune suppressive TAMs resulting in T-cell anergy. In extra-pancreatic disease, radiation-induced vascular damage with subsequent release of HIF-1α and SDF-1 results in the recruitment of macrophages to the TME via CXCR4

ligation[35, 36]. By contrast, we show that in PDA, RT-induced M-CSF expression is a primary mechanism which drives TAM infiltration. This also results in preferential M2 polarization, including diminished MHC II expression, up-regulation of Arg1, and high expression of macrophage scavenger receptor 1 (MSR1; CD204) and the mannose receptor (CD206). Increased expression of the enzyme Arginase 1 can deplete L-arginine which is vital for proper T cell function[37, 38]. More importantly, our experiments suggest that RT-recruited macrophages substantially influence the profile of tumor infiltrating lymphocytes in PDA, shifting the balance in favor of IL-10 producing Th2 cells and Tregs, and decreasing the CD8:CD4 T cell ratio. Collectively, our post-RT immune-phenotyping analyses suggest a predominance of tumor-promoting $CD4^+$ T cell subsets within the TME after RT-induced immune reprogramming, as well as an anergic phenotype in the remaining $CD8^+$ effector T cells. Moreover, our T cell adoptive transfer experiments imply that the principal tumor-promoting effect of RT may relate to the accumulation of Tregs given the observation that RT-entrained T cells harvested from orthotopic KPC tumors can even promote accelerated growth of Pan02 tumors, suggesting lack of antigen specificity.

Radiation-induced recruitment of M2-polarized TAMs appears to be dependent on the precise experimental model employed. Deng et al. recently found a decrease in the number of myeloid cells in the TUBO mammary carcinoma and MC38 colon carcinoma models 3 days after a combined treatment of a single RT fraction (12 Gy) and immunotherapy[39]. Klug et al reported that doses of RT of ≤ 2 Gy actually polarized TAMs toward an M1 phenotype with increased production of iNOS[40]. This observation is consistent with data from experiments using lower doses of RT on peritoneal macrophages *in vitro*[41]. However, data from a diversity of other tumor models suggest that radiation can drive infiltration of M2-polarized TAMs[35, 42, 43]. It is notable that RT effects on TAM recruitment and M2-polarization were only observed at early time points after RT but absent at 8 weeks suggesting that the inflammatory stimulus for TAM recruitment and programming may dissipate at later time points. Indeed, we found that by M-CSF expression reduced to baseline levels by 8 weeks post-RT.

The incapacitating effects of TAMs on adaptive anti-tumor immunity in the context of radiation treatment of PDA become more salient in light of the consequences of macrophage inhibition. M-CSF or F4/80 neutralization in combination with RT increased the radiation effect on tumor control as evidenced by a ~2-fold diminished tumor volume compared with either treatment alone. Furthermore, α-M-CSF treatment reduced TAM infiltration, lowered their expression of CD204 and CD206 but increased MHC-II, and resulted in immunogenic reprogramming of $CD4^+$ and $CD8^+$ T-cells suggesting that M2-deviated TAMs are orchestrators of T-cell anergy after irradiation of PDA. Our findings are in consort with a very recent report in murine breast cancer models where macrophage depletion significantly delayed tumor regrowth following radiotherapy[44]. Notably, despite lowering TAM infiltration, αM-CSF alone does not have tumor-protective effects *in vivo* when not combined with RT. This is likely related to the fact that at baseline, in absence of RT, TAMs are not overwhelmingly M2-polarized in PDA.

Besides directing $CD4^+$ T cell differentiation toward a Th2 or Treg phenotype, tumor-infiltrating myeloid cells can induce apoptosis or exhaustion in tumor-specific CTLs via PD-

L1–PD1 ligation[45]. We show that RT induces upregulation of PD-L1 in PDA-infiltrating TAMs, which is potentially another mode of immune suppression that can account for radio-resistance in PDA. Indeed, Twyman-Saint Victor et al. reported that RT alone has only modest efficacy in PDA cell lines implanted in the flank, but combination therapy with PD-1 and CTLA4 inhibition offers impressive tumor protection[46]. Similarly, in models of colorectal and breast cancer, RT has been shown to upregulate PD-L1 on myeloid cells, whereas the efficacy of radiation is synergistically enhanced when combined with blockade of the PD-L1-PD1 axis[39]. These reports highlight a fundamental and seemingly paradoxical principal of immunotherapy: accentuating immune suppression by RT-induced upregulation of PD-L1 can enhance the therapeutic efficacy of immunotherapeutics targeting PD-L1 or PD1. Similarly, our data imply that whereas α-M-CSF or α-F4/80 immunotherapies have only modest efficacy in absence of RT, they each impressively diminished tumor growth when combined with RT. Hence, RT may enhance the therapeutic efficacy of immunotherapy not only via the mechanisms discussed above, but also through modulation of the immune contexture of the TME which provides targets for immunotherapeutic manipulation. Altogether, our data imply that M-CSF blockade should be tested in clinical trials as an adjuvant to enhance the efficacy of RT in patients with locally advanced unresectable PDA.

Supplementary Material

Refer to Web version on PubMed Central for supplementary material.

Acknowledgments

Grant Support: This work was supported in-part by grants for the German Research Foundation (LS), the Schwartz Fellowship in GI Oncology (DD), the Lustgarten Foundation (GM), the Pancreatic Cancer Action Network (GM), and National Institute of Health Awards CA155649 (GM), and CA168611 (GM).

References

1. Jemal A, Siegel R, Xu J, et al. Cancer statistics, 2010. CA Cancer J Clin. 2010; 60:277–300. [PubMed: 20610543]
2. Conlon KC, Klimstra DS, Brennan MF. Long-term survival after curative resection for pancreatic ductal adenocarcinoma. Clinicopathologic analysis of 5-year survivors. Ann Surg. 1996; 223:273–279. [PubMed: 8604907]
3. Butturini G, Stocken DD, Wente MN, et al. Influence of resection margins and treatment on survival in patients with pancreatic cancer: meta-analysis of randomized controlled trials. Arch Surg. 2008; 143:75–83. discussion 83. [PubMed: 18209156]
4. Neoptolemos JP, Stocken DD, Friess H, et al. A randomized trial of chemoradiotherapy and chemotherapy after resection of pancreatic cancer. N Engl J Med. 2004; 350:1200–1210. [PubMed: 15028824]
5. Moertel CG, Frytak S, Hahn RG, et al. Therapy of locally unresectable pancreatic carcinoma: a randomized comparison of high dose (6000 rads) radiation alone, moderate dose radiation (4000 rads + 5-fluorouracil), and high dose radiation + 5-fluorouracil: The Gastrointestinal Tumor Study Group. Cancer. 1981; 48:1705–1710. [PubMed: 7284971]
6. Klaassen DJ, MacIntyre JM, Catton GE, et al. Treatment of locally unresectable cancer of the stomach and pancreas: a randomized comparison of 5-fluorouracil alone with radiation plus concurrent and maintenance 5-fluorouracil--an Eastern Cooperative Oncology Group study. J Clin Oncol. 1985; 3:373–378. [PubMed: 3973648]

7. Treatment of locally unresectable carcinoma of the pancreas: comparison of combined-modality therapy (chemotherapy plus radiotherapy) to chemotherapy alone. Gastrointestinal Tumor Study Group. J Natl Cancer Inst. 1988; 80:751–755. [PubMed: 2898536]
8. Chauffert B, Mornex F, Bonnetain F, et al. Phase III trial comparing intensive induction chemoradiotherapy (60 Gy, infusional 5-FU and intermittent cisplatin) followed by maintenance gemcitabine with gemcitabine alone for locally advanced unresectable pancreatic cancer. Definitive results of the 2000-01 FFCD/SFRO study. Ann Oncol. 2008; 19:1592–1599. [PubMed: 18467316]
9. Loehrer PJ, Powell ME, Cardenes HR, et al. A randomized phase III study of gemcitabine in combination with radiation therapy versus gemcitabine alone in patients with localized, unresectable pancreatic cancer: E4201. J Clin Oncol. 2008 Abstract 4506.
10. Wang F, Kumar P. The role of radiotherapy in management of pancreatic cancer. J Gastrointest Oncol. 2011; 2:157–167. [PubMed: 22811846]
11. Hazard L. The role of radiation therapy in pancreas cancer. Gastrointest Cancer Res. 2009; 3:20–28. [PubMed: 19343134]
12. Hruban RH, Maitra A, Goggins M. Update on pancreatic intraepithelial neoplasia. Int J Clin Exp Pathol. 2008; 1:306–316. [PubMed: 18787611]
13. Korc M. Pancreatic cancer-associated stroma production. American journal of surgery. 2007; 194:S84–S86. [PubMed: 17903452]
14. Miyamoto H, Murakami T, Tsuchida K, et al. Tumor-stroma interaction of human pancreatic cancer: acquired resistance to anticancer drugs and proliferation regulation is dependent on extracellular matrix proteins. Pancreas. 2004; 28:38–44. [PubMed: 14707728]
15. De Monte L, Reni M, Tassi E, et al. Intratumor T helper type 2 cell infiltrate correlates with cancer-associated fibroblast thymic stromal lymphopoietin production and reduced survival in pancreatic cancer. J Exp Med. 2011; 208:469–478. [PubMed: 21339327]
16. Fukunaga A, Miyamoto M, Cho Y, et al. CD8+ tumor-infiltrating lymphocytes together with CD4+ tumor-infiltrating lymphocytes and dendritic cells improve the prognosis of patients with pancreatic adenocarcinoma. Pancreas. 2004; 28:e26–e31. [PubMed: 14707745]
17. Hiraoka N, Onozato K, Kosuge T, et al. Prevalence of FOXP3+ regulatory T cells increases during the progression of pancreatic ductal adenocarcinoma and its premalignant lesions. Clin Cancer Res. 2006; 12:5423–5434. [PubMed: 17000676]
18. Ochi A, Nguyen AH, Bedrosian AS, et al. MyD88 inhibition amplifies dendritic cell capacity to promote pancreatic carcinogenesis via Th2 cells. J Exp Med. 2012; 209:1671–1687. [PubMed: 22908323]
19. Pylayeva-Gupta Y, Lee KE, Hajdu CH, et al. Oncogenic Kras-induced GM-CSF production promotes the development of pancreatic neoplasia. Cancer cell. 2012; 21:836–847. [PubMed: 22698407]
20. Connolly MK, Mallen-St Clair J, Bedrosian AS, et al. Distinct populations of metastases-enabling myeloid cells expand in the liver of mice harboring invasive and preinvasive intra-abdominal tumor. J Leukoc Biol. 2010; 87:713–725. [PubMed: 20042467]
21. Liu CY, Xu JY, Shi XY, et al. M2-polarized tumor-associated macrophages promoted epithelial-mesenchymal transition in pancreatic cancer cells, partially through TLR4/IL-10 signaling pathway. Lab Invest. 2013; 93:844–854. [PubMed: 23752129]
22. Hingorani SR, Petricoin EF, Maitra A, et al. Preinvasive and invasive ductal pancreatic cancer and its early detection in the mouse. Cancer Cell. 2003; 4:437–450. [PubMed: 14706336]
23. Hingorani SR, Wang L, Multani AS, et al. Trp53R172H and KrasG12D cooperate to promote chromosomal instability and widely metastatic pancreatic ductal adenocarcinoma in mice. Cancer Cell. 2005; 7:469–483. [PubMed: 15894267]
24. Carriere C, Young AL, Gunn JR, et al. Acute pancreatitis markedly accelerates pancreatic cancer progression in mice expressing oncogenic Kras. Biochem Biophys Res Commun. 2009; 382:561–565. [PubMed: 19292977]
25. Ochi A, Graffeo CS, Zambirinis CP, et al. Toll-like receptor 7 regulates pancreatic carcinogenesis in mice and humans. J Clin Invest. 2012; 122:4118–4129. [PubMed: 23023703]

26. Hruban RH, Adsay NV, Albores-Saavedra J, et al. Pancreatic intraepithelial neoplasia: a new nomenclature and classification system for pancreatic duct lesions. Am J Surg Pathol. 2001; 25:579–586. [PubMed: 11342768]
27. Lacey DC, Achuthan A, Fleetwood AJ, et al. Defining GM-CSF- and macrophage-CSF-dependent macrophage responses by in vitro models. J Immunol. 2012; 188:5752–5765. [PubMed: 22547697]
28. Werthmoller N, Frey B, Wunderlich R, et al. Modulation of radiochemoimmunotherapy-induced B16 melanoma cell death by the pan-caspase inhibitor zVAD-fmk induces anti-tumor immunity in a HMGB1-, nucleotide- and T-cell-dependent manner. Cell Death Dis. 2015; 6:e1761. [PubMed: 25973681]
29. Panaretakis T, Joza N, Modjtahedi N, et al. The co-translocation of ERp57 and calreticulin determines the immunogenicity of cell death. Cell Death Differ. 2008; 15:1499–1509. [PubMed: 18464797]
30. Ogden CA, deCathelineau A, Hoffmann PR, et al. C1q and mannose binding lectin engagement of cell surface calreticulin and CD91 initiates macropinocytosis and uptake of apoptotic cells. J Exp Med. 2001; 194:781–795. [PubMed: 11560994]
31. Gudkov AV, Komarova EA. The role of p53 in determining sensitivity to radiotherapy. Nat Rev Cancer. 2003; 3:117–129. [PubMed: 12563311]
32. Ghiringhelli F, Apetoh L, Tesniere A, et al. Activation of the NLRP3 inflammasome in dendritic cells induces IL-1beta-dependent adaptive immunity against tumors. Nat Med. 2009; 15:1170–1178. [PubMed: 19767732]
33. Ma Y, Aymeric L, Locher C, et al. Contribution of IL-17-producing gamma delta T cells to the efficacy of anticancer chemotherapy. J Exp Med. 2011; 208:491–503. [PubMed: 21383056]
34. Rosental B, Appel MY, Yossef R, et al. The effect of chemotherapy/radiotherapy on cancerous pattern recognition by NK cells. Curr Med Chem. 2012; 19:1780–1791. [PubMed: 22414084]
35. Chiang CS, Fu SY, Wang SC, et al. Irradiation promotes an m2 macrophage phenotype in tumor hypoxia. Front Oncol. 2012; 2:89. [PubMed: 22888475]
36. Ceradini DJ, Kulkarni AR, Callaghan MJ, et al. Progenitor cell trafficking is regulated by hypoxic gradients through HIF-1 induction of SDF-1. Nat Med. 2004; 10:858–864. [PubMed: 15235597]
37. Fletcher M, Ramirez ME, Sierra RA, et al. l-Arginine depletion blunts antitumor T-cell responses by inducing myeloid-derived suppressor cells. Cancer Res. 2015; 75:275–283. [PubMed: 25406192]
38. Rodriguez PC, Quiceno DG, Zabaleta J, et al. Arginase I production in the tumor microenvironment by mature myeloid cells inhibits T-cell receptor expression and antigen-specific T-cell responses. Cancer Res. 2004; 64:5839–5849. [PubMed: 15313928]
39. Deng L, Liang H, Burnette B, et al. Irradiation and anti-PD-L1 treatment synergistically promote antitumor immunity in mice. J Clin Invest. 2014; 124:687–695. [PubMed: 24382348]
40. Klug F, Prakash H, Huber PE, et al. Low-dose irradiation programs macrophage differentiation to an iNOS(+)/M1 phenotype that orchestrates effective T cell immunotherapy. Cancer Cell. 2013; 24:589–602. [PubMed: 24209604]
41. Chiang CS, Chen FH, Hong JH, et al. Functional phenotype of macrophages depends on assay procedures. Int Immunol. 2008; 20:215–222. [PubMed: 18096562]
42. Crittenden MR, Cottam B, Savage T, et al. Expression of NF-kappaB p50 in tumor stroma limits the control of tumors by radiation therapy. PLoS One. 2012; 7:e39295. [PubMed: 22761754]
43. Coates PJ, Rundle JK, Lorimore SA, et al. Indirect macrophage responses to ionizing radiation: implications for genotype-dependent bystander signaling. Cancer Res. 2008; 68:450–456. [PubMed: 18199539]
44. Shiao SL, Ruffell B, DeNardo DG, et al. TH2-Polarized CD4+ T Cells and Macrophages Limit Efficacy of Radiotherapy. Cancer Immunol Res. 2015; 3:518–525. [PubMed: 25716473]
45. Pilones KA, Vanpouille-Box C, Demaria S. Combination of radiotherapy and immune checkpoint inhibitors. Semin Radiat Oncol. 2015; 25:28–33. [PubMed: 25481263]
46. Twyman-Saint Victor C, Rech AJ, Maity A, et al. Radiation and dual checkpoint blockade activate non-redundant immune mechanisms in cancer. Nature. 2015; 520:373–377. [PubMed: 25754329]

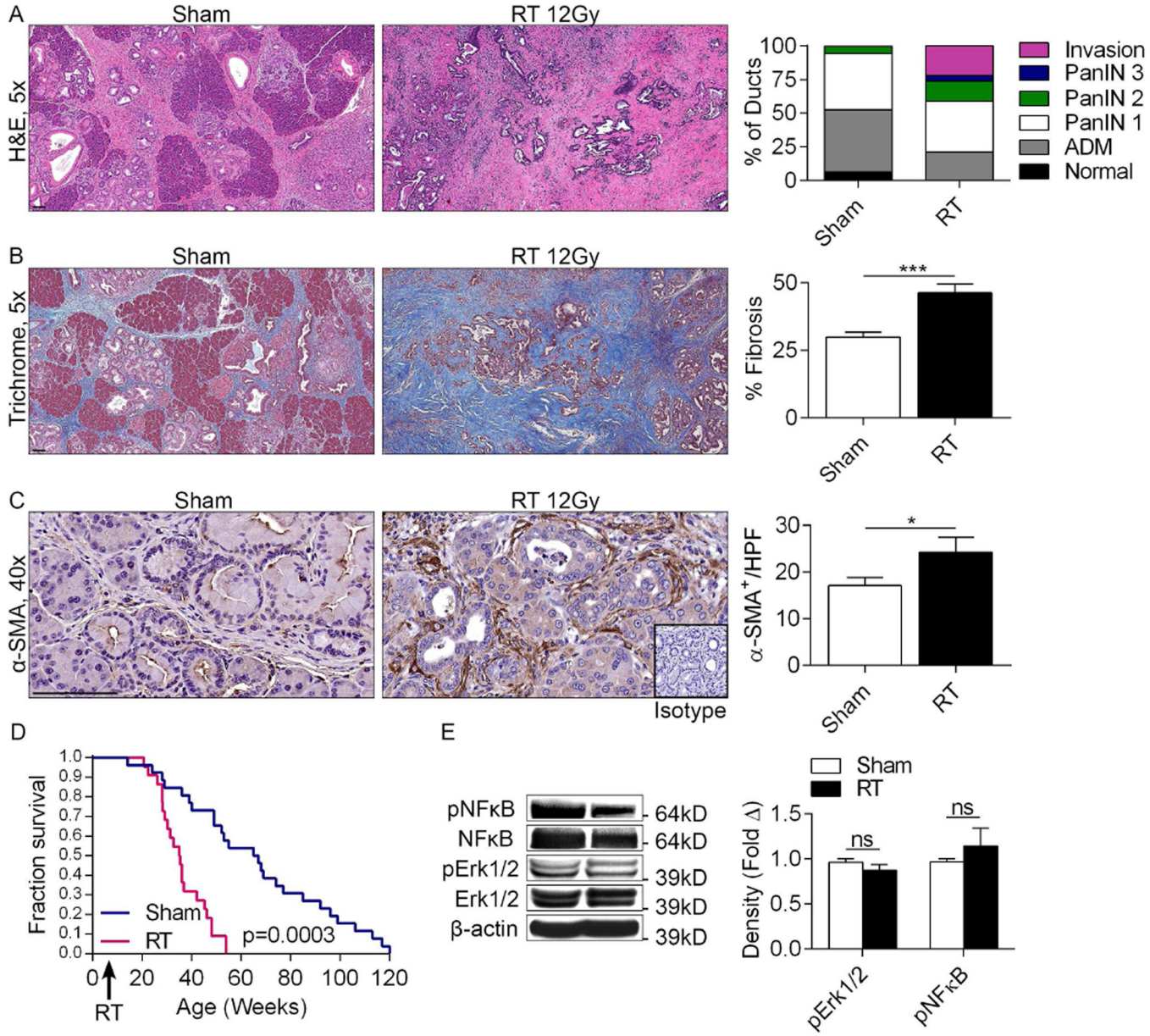

Figure 1. RT accelerates the rate of pancreatic oncogenesis in the context of pre-invasive disease

(a) KC mice underwent pancreas-directed RT or sham treatment at 6 weeks of life and pancreata were assayed 8 weeks later (n=10/group). Pancreas sections were examined by H&E and the fractions of normal ducts, acinoductal metasplasia (ADM), PanIN I-III lesions, and invasive cancer were quantified. **(b)** Fibrosis was quantified using Trichrome staining. **(c)** Pancreatic stellate cell activation was determined by α-SMA staining. **(d)** KC mice underwent pancreas-directed RT (n=22) or sham treatment (n=29) at 6 weeks of life. Kaplan-Meier survival analysis was performed. **(e)** Activation of NF-κB and MAP kinase siganling in RT-treated and control pancreata was determined by western blotting. Representative data and summary of triplicates are shown (*p<0.05, ***p<0.001).

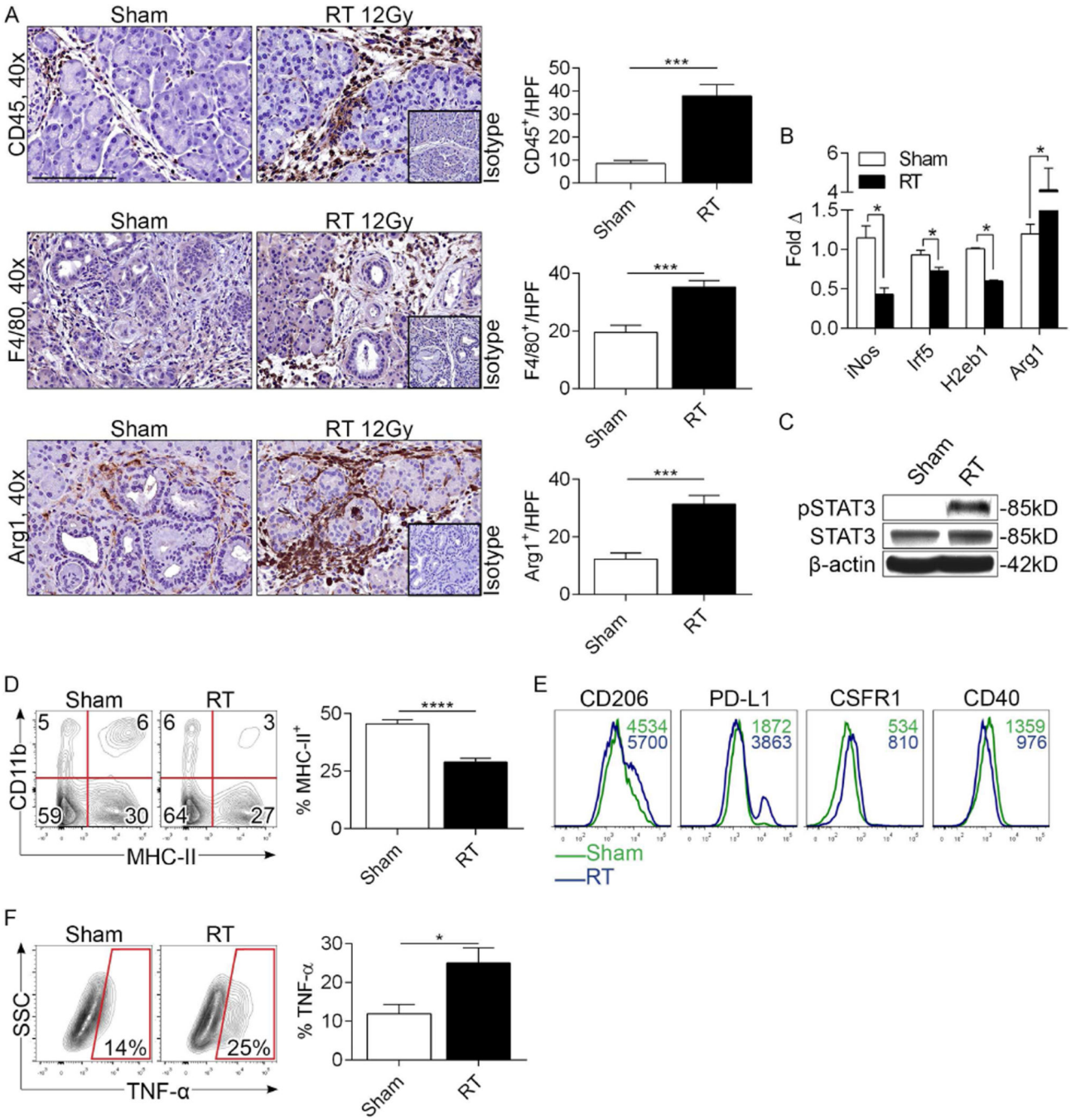

Figure 2. RT increases TAM infiltration and induces M2-polarization in pre-invasive PDA

(a) KC mice underwent pancreas-directed RT or sham treatment at 6 weeks of life and pancreata were assayed 3 days later (n=10/group). IHC on paraffin-embedded pancreatic sections was performed using mAbs directed against $CD45^+$-pan leukocytes, $F480^+$ cells, and $Arg1^+$ cells. Cellular infiltrates were quantified by examining 10 HPFs per slide. **(b)** mRNA levels of iNos, Irf5, H2Eb1, and Arg1 were tested in RT- or sham-treated pancreata by nanostring assay. **(c)** STAT3 phosphorylation was evaluated by western blotting. **(d)** $Gr1^-F4/80^+$ cells in sham- and RT-treated pancreata from KC mice were gated and tested for

co-expression of CD11b and MHCII. The fraction of $Gr1^{-}F4/80^{+}CD11b^{+}$ TAMs expressing MHCII was quantified. **(e)** $Gr1^{-}F4/80^{+}CD11b^{+}$ TAMs from sham or RT-treated KC pancreata were gated by flow cytometry and tested for expression of CD206, PD-L1, CSFR1, and CD40. Representative histogram overlays are shown. MFIs are indicated for each respective treatment group. **(f)** TNF-α expression was determined in $Gr1^{-}F4/80^{+}CD11b^{+}$ TAMs from sham- and RT-treated pancreata. Flow cytometry experiments were performed using 3-5 mice per arm and reproduced more than 5 times (*$p<0.05$, ***$p<0.001$, ****$p<0.001$).

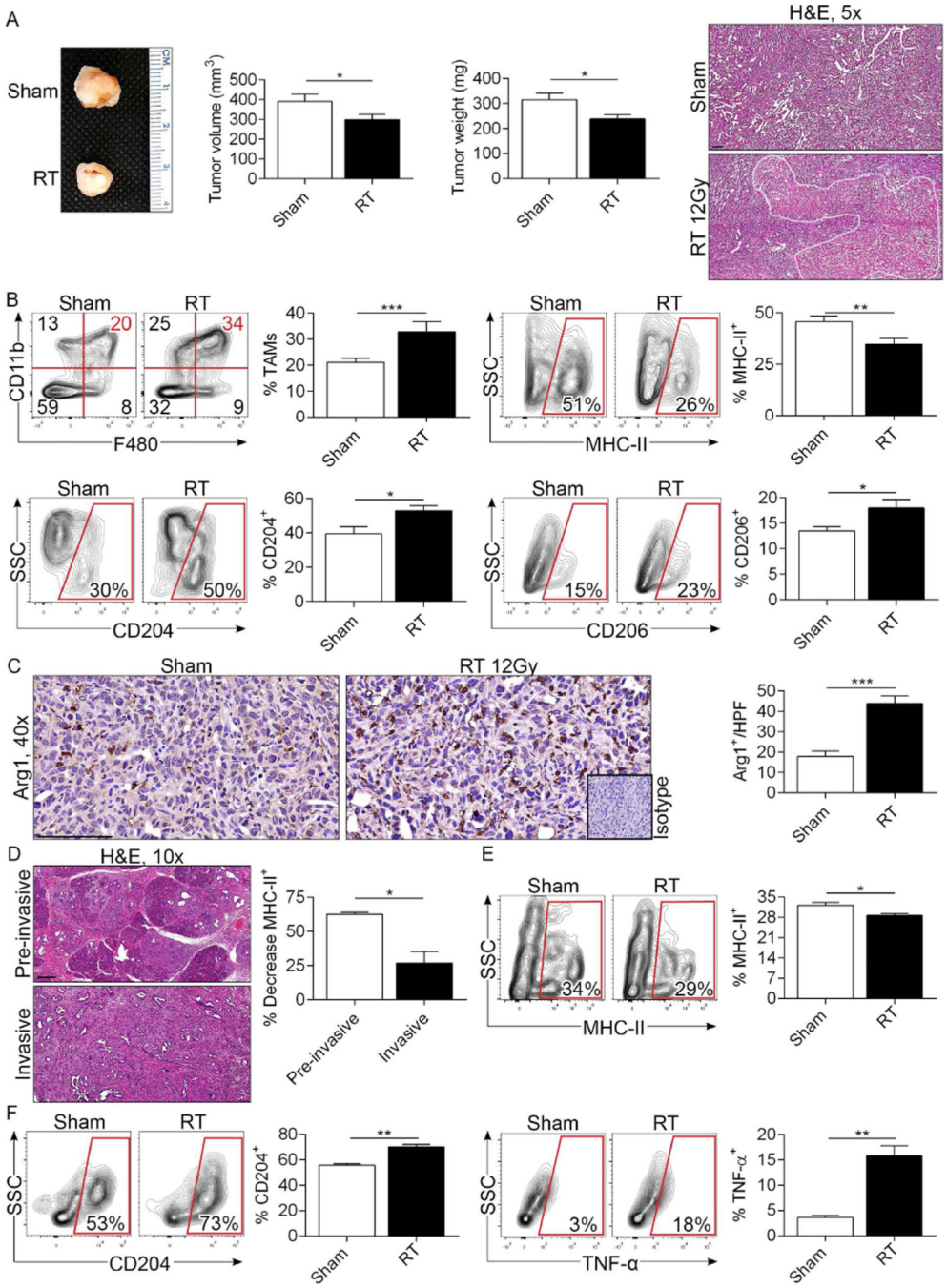

Figure 3. RT increases infiltration of TAMs and induces M2-like polarization in invasive PDA

(a) WT mice were orthotopically implanted with KPC-derived tumors and cohorts were treated with tumor-focused RT or sham-treated at 18 days. Pancreatic tumors were harvested on day 21. Representative gross pictures of tumors and quantitative data on tumor volume and weight are shown (n=15/cohort). Representative H&E stained images are shown and necrotic areas bracketed. **(b)** The fraction of $Gr1^{-}F4/80^{+}CD11b^{+}$ TAMs among $CD45^{+}$ leukocytes in the tumor microenvironment was determined by flow cytometry. TAMs were then gated and tested for expression of MHC II, CD204, and CD206. Representative contour

plots and summary data are shown. **(c)** $Arg1^+$ cellular infiltration in sham- and RT-treated KPC-derived orthotopic tumors was determined by IHC. **(d)** MHCII expression was tested in TAMs from disparate areas of RT-treated KPC mice by separately examining areas with invasive carcinoma or pre-invasive lesions. The percent decrease in MHCII expression in TAMs after RT treatment was calculated for invasive and pre-invasive lesions, respectively (n=3). **(e)** Splenic macrophages were co-cultured with sham-treated or irradiated (20 Gy) KPC-derived tumor cells (2:1 ratio) in quadruplicate. After 48 hours of co-culture, macrophages were harvested and analyzed for expression of MHC II, **(f)** CD204, and TNF-α. *In vitro* experiments were repeated at least 3 times with similar results (*p<0.05, **p<0.01, ***p<0.001).

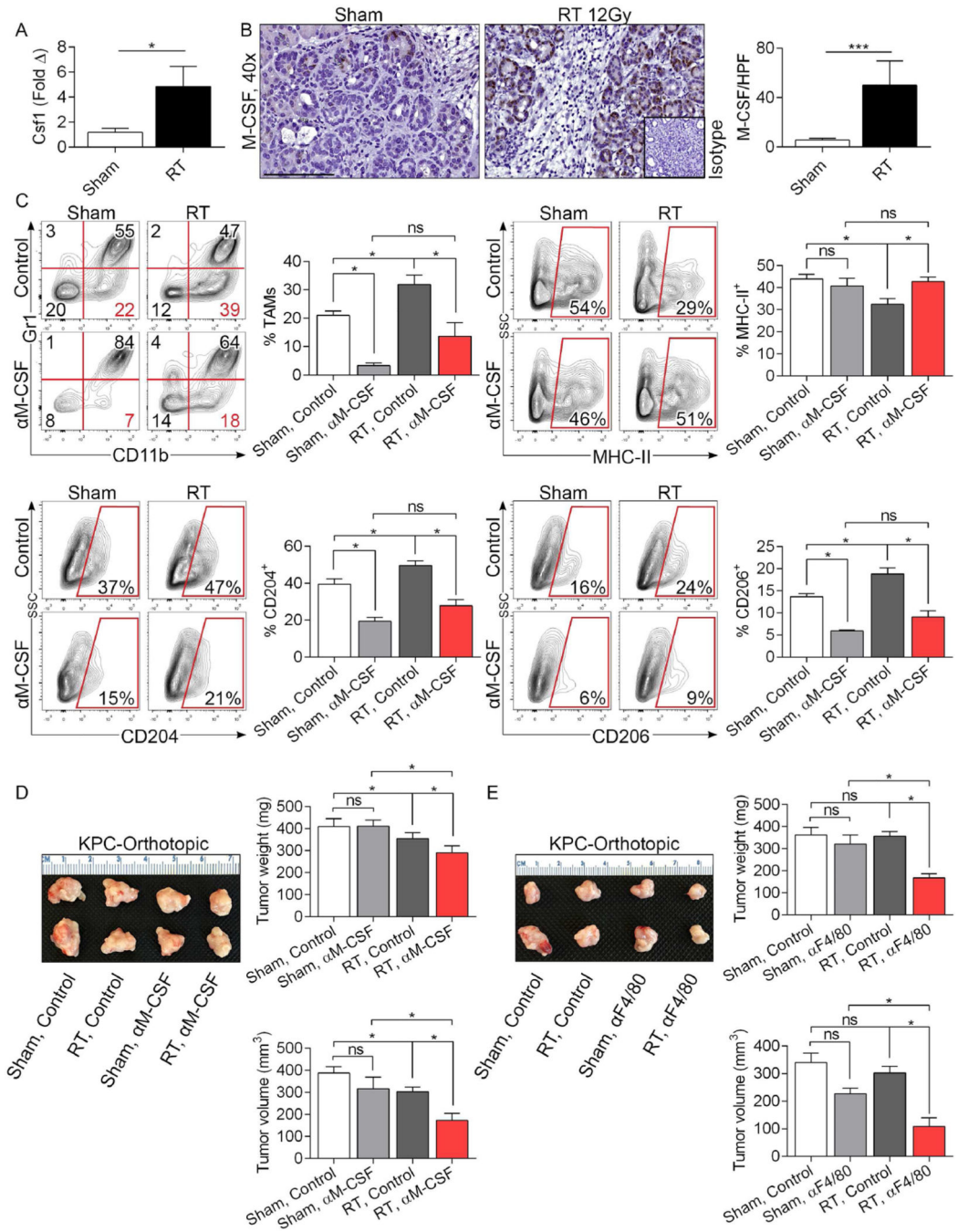

Figure 4. M-CSF blockade mitigates the M2 macrophage reprogramming associated with RT and enhances the efficacy of therapy

(a) qPCR for *CSF1* was performed on RT- and sham-treated orthotopic PDA tumors on day 3 after RT (n=3/group). **(b)** IHC for M-CSF was performed on day 3 in pancreata of irradiated and sham-treated KC mice (n=3/group). **(c, d)** WT mice were orthotopically implanted with KPC-derived tumors and cohorts were treated with tumor-focused RT or sham-treated at 18 days. Select cohorts were additionally treated with a neutralizing α-M-CSF mAb. Mice were sacrificed on day 21 and tested for the fraction of tumor-infiltrating

$Gr1^{-}F480^{+}CD11b^{+}$ TAMs. Further, TAMs were then gated and tested for MHCII, CD204, and CD206 expression. **(d)** Representative photographs of PDA tumors, average tumor weights, and tumor volumes are shown (n=12/group). **(e)** WT mice were orthotopically implanted with KPC-derived tumors and cohorts were treated with tumor-focused RT or sham-treated as above. Select cohorts were additionally treated with a neutralizing α-F4/80 mAb. Representative photographs of PDA tumors, average tumor weights, and tumor volumes are shown (n=9/group; *$p<0.05$, ***$p<0.001$).

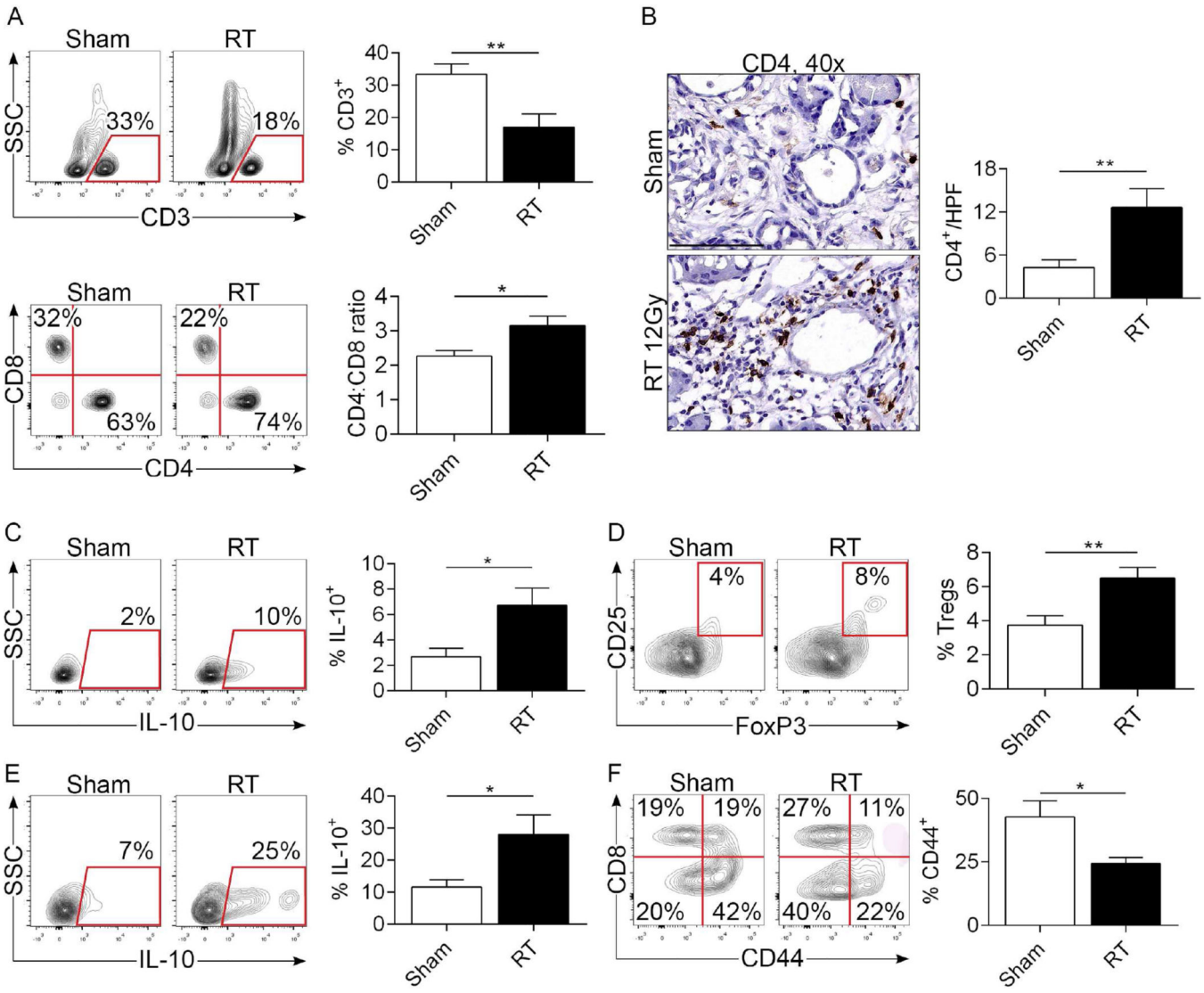

Figure 5. RT induces an immune suppressive T cell profile in PDA

(a) KC mice underwent pancreas-directed RT or sham-treatment at 6 weeks of life and pancreata were assayed 3 days later (n=10/group). The percentage of $CD3^+$ T cells within the inflammatory TME and the CD4:CD8 T cell ratio were determined by flow cytometry. **(b)** The total number of pancreas-infiltrating $CD4^+$ T cells was assessed by IHC in both the RT- and sham-treated cohorts. **(c)** IL-10 expression on pan-$CD4^+$ T cells was determined by intracellular cytokine staining (ICC). **(d)** Treg differentiation was determined by co-expression of CD25 and FoxP3 in $CD4^+$ T cells. **(e)** IL-10 expression in Tregs was assayed by ICC. **(f)** $CD8^+$ T cells were tested for expression of CD44 in sham-versus RT-treated pancreata of KC mice (*p<0.05, **p<0.01).

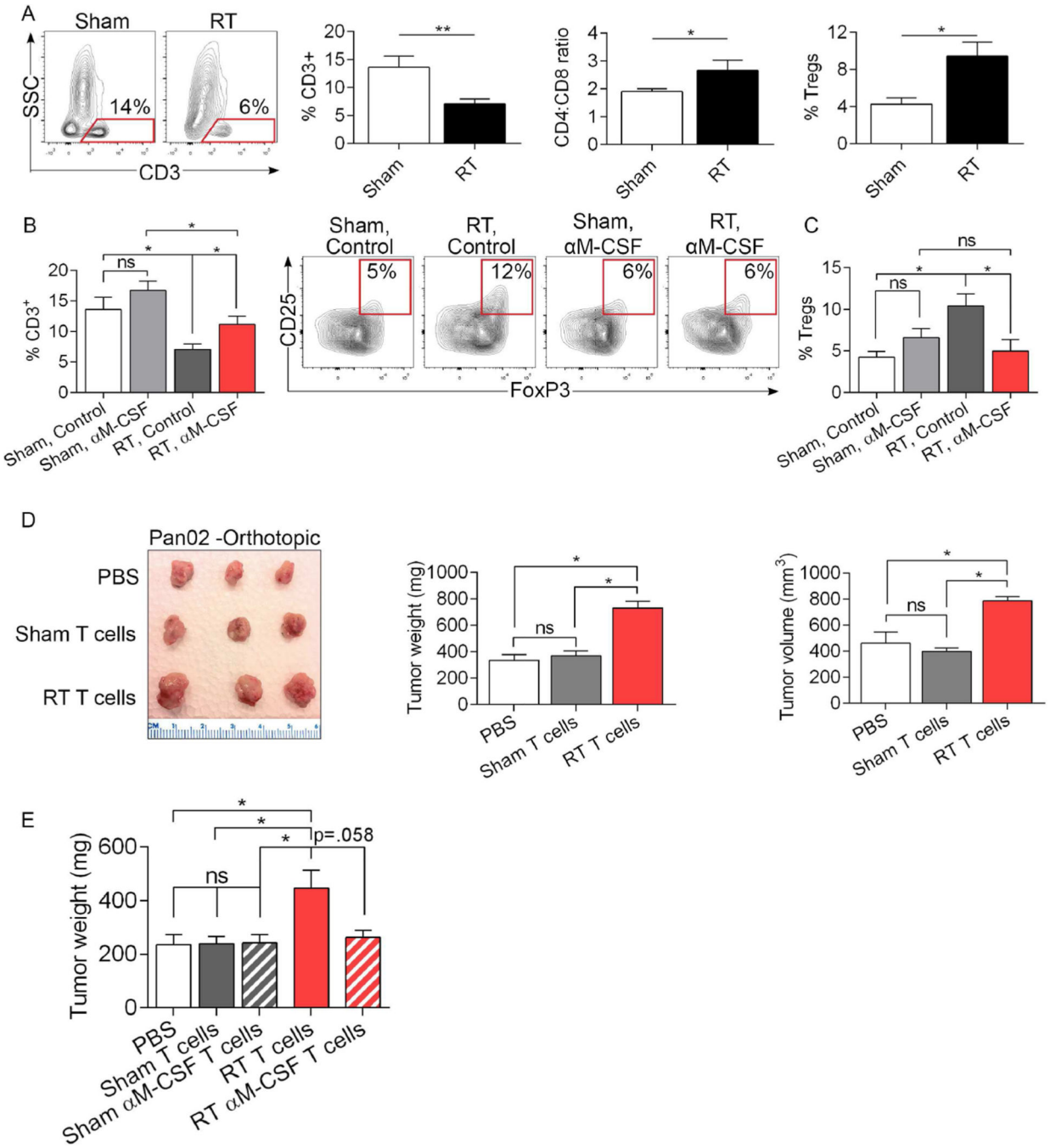

Figure 6. RT programs tumor-infiltrating T cells in invasive PDA into tumor promoting entities in an M-CSF dependent manner

(a) Sham- or RT-treated orthotopic KPC-derived tumors were assayed on day 3 after treatment for the fraction of tumor-infiltrating $CD3^+$ T cells, the CD4:CD8 T cell ratio, and the fraction of tumor-infiltrating Tregs. **(b)** Select cohorts of sham- or RT-treated orthotopic KPC-derived tumors were additionally treated with a neutralizing α-M-CSF mAb and tested for the fraction of tumor-infiltrating $CD3^+$ T cells and **(c)** $CD4^+CD25^+FoxP3^+$ Tregs on day 3 after treatment (n=10/group; *p<0.05, **p<0.01). **(d)** WT mice were administered a

subcutaneous injection of Pan02-derived tumor + PBS, Pan02 cells + T cells harvested from day 21 sham-treated orthotopic KPC-derived PDA (10:1 ratio), or Pan02 cells + T cells harvested from RT-treated PDA. Animals were sacrificed on day 35 and subcutaneous tumors harvested. Representative images of tumors from each treatment cohort, average tumor weight, and tumor volume are shown (n=5/cohort). **(e)** WT mice were administered a subcutaneous injection of KPC-derived tumor cells + PBS, KPC cells + T cells harvested from sham-treated KPC-derived PDA (10:1 ratio), KPC cells + T cells harvested from αM-CSF-treated PDA, KPC cells + T cells harvested from RT-treated PDA, or KPC cells + T cells harvested from αM-CSF + RT-treated PDA. Animals were sacrificed at day 17 and subcutaneous tumors were weighed (n=5/cohort; *$p<0.05$).